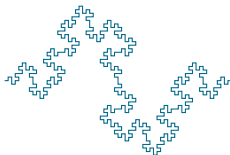


Accurate MR Restoration with Correction for Intensity Inhomogeneity

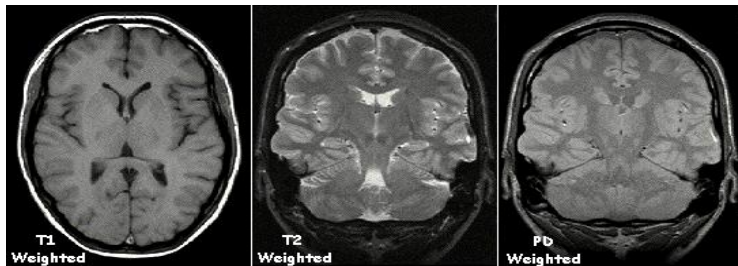
Yuping Duan

Center for Applied Mathematics of Tianjin University



April 14, 2018

MAGNETIC RESONANCE IMAGING (MRI)



Magnetic Resonance Imaging (MRI) is a medical imaging technique used in radiology to form pictures of the anatomy and the physiological processes of the body in both health and disease.

Two main degradation of MRI:

- Intensity Inhomogeneity
- Noises

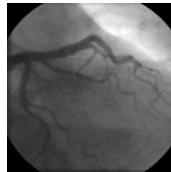
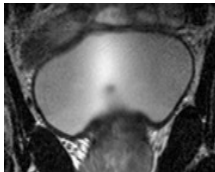
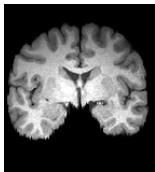
INTENSITY INHOMOGENEITY

- Intensity inhomogeneity occurs in many real world images from different modalities, such as

x-ray radiography, ultrasonic techniques, magnetic resonance (MR) images etc..

- Intensity inhomogeneity may be caused by following sources for MRI
B1 and B0 field inhomogeneity, poor radio frequency (RF) coil uniformity and patient anatomy both inside and outside the field of view etc..

Note: Intensity inhomogeneity may severely challenge the image segmentation algorithms!



INTENSITY INHOMOGENEITY

- Decomposition models for images with intensity inhomogeneity:

- Model I (D.L. Pham and J.L. Prince'99)

$$f(x) = u(x)b(x) + n(x)$$

- Model II (S. Prima et al'01, J. Ashburner et al'05)

$$f(x) = (u(x) + n(x))b(x)$$

- Model III (W.M. Wells et al'96, K.V. Leemput et al'99)

$$\log f(x) = \log u(x) + \log b(x) + n(x)$$

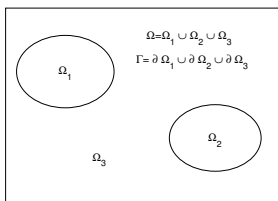
- Assumptions:

- **u is a piecewise constant function** → true intensity
- **b is a spatially smooth function** → bias field
- n follows the Gaussian distribution → **Not true for MRI**

METHODOLOGIES FOR BIAS CORRECTION

- Bias field estimation via the data
 - Nonparametric nonuniformity normalization (N3) algorithm (J.G. Sled et al'98)
 - N4ITK algorithm (N.J. Tustison et al'10)
 - Entropy-related method (J.V. Manjon et al'07)
 - Many others ...
- Bias field estimation in a segmentation process
 - Fuzzy c-means method (D.L. Pham and J.L. Prince'99) , (M.N. Ahmed et al'02), etc.
 - **Chan-Vese model / Mumford-Shah model**

MUMFORD-SHAH MODEL (89')



- The **Mumford-Shah model** (D. Mumford and J. Shah'89) is one of the most important variational image segmentation model, which is defined as

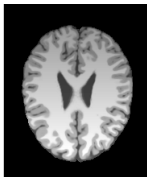
$$\min_{u, \Gamma} \left\{ E_{MS}(u, \Gamma) := \int_{\Omega} |v - u|^2 dx + \frac{\mu}{2} \int_{\Omega \setminus \Gamma} |\nabla u|^2 dx + \alpha |\Gamma| \right\},$$
$$\Gamma = \cup_{i=1}^m \partial \Omega_i, \quad \Omega = \cup_{i=1}^m \Omega_i \quad \text{s.t.} \quad \Omega_k \cap \Omega_l = \emptyset, \quad \forall k \neq l.$$

Comments: The first term imposes the condition that u is smooth in the region $\Omega \setminus \Gamma$, the second measures the fidelity to the data, and the third term establishes that the discontinuity set has minimal length and therefore is as smooth as possible.

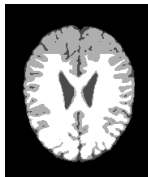
- Discontinuities in the domain ($\Omega \setminus \Gamma, \Gamma$) make minimization difficult**

PIECEWISE-CONSTANT MS MODELS

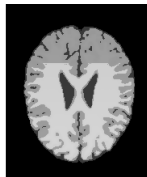
- Chan-Vese model (T. Chan and L. Vese'01), Vese-Chan model (L. Vese and T. Chan'02)
- Convexified CV model (T. Chan et al'06), (X. Bresson et al'07)
- Convexified multi-phase labeling/segmentation models (E. Bae et al'11), (Y. Gu et al'12), (X. Cai et al'13)



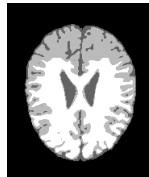
(a) Input



(b) Bae



(c) Gu



(d) Cai

PIECEWISE-SMOOTH MS MODELS

- The so-called local intensity fitting energy is defined as

$$\mathcal{E}(C, u_1, u_2) = \sum_{i=1}^2 \lambda_i \int_{\Omega_i} K(x-y) |v(y) - u_i(x)|^2 dy,$$

where K is a nonnegative kernel function $K : \mathbb{R}^n \rightarrow [0, +\infty)$ satisfying:

- 1) $K(-u) = K(u)$;
 - 2) $K(u) \geq K(v)$, if $|u| < |v|$, and $\lim_{|u| \rightarrow \infty} K(u) = 0$;
 - 3) $\int K(x) dx = 1$.
- The CV model is rewritten as (Li et al '07)

$$\min_{C, u_1, u_2} \int_{\Omega} \mathcal{E}(C, u_1(x), u_2(x)) dx + \alpha |C|$$

PIECEWISE-SMOOTH MS MODELS

- The multi-phase Mumford-Shah model can be rewritten as follows

$$\min_{\{u_i, \Omega_i\}_{i=1}^n} \sum_{i=1}^N \left(\alpha |\partial \Omega_i| + \frac{\mu}{2} \int_{\Omega_i} |\nabla u_i|^2 dx + \int_{\Omega_i} |u_i - v|^2 dx \right)$$

- u_i can be solved by gradient descent flow as

$$\frac{\partial u_i}{\partial t} = \mu \Delta u_i - (u_i - v) \quad \text{in } \Omega_i \implies \begin{cases} \frac{\partial u_i}{\partial t} = \mu \Delta u_i & \text{in } \Omega_i, \\ u_i|_{t=0} = v. \end{cases}$$

the solution of which is

$$u_i = G_\sigma * v = \int_{\mathbb{R}^2} G_\sigma(x - y) v(y) dy.$$

- The multi-phase MS model with local binary fitting energy is defined as
(Gu et al '17)

$$\min_{\{u_i, \Omega_i\}_{i=1}^n} \sum_{i=1}^n \left(\alpha |\partial \Omega_i| + \frac{\mu}{2} \iint_{\Omega_i \times \Omega_i} K(x - y) |v(y) - u_i(x)|^2 dy dx \right),$$

where K is a general smoothing operator.

PIECEWISE-SMOOTH MS MODELS

- Define a piecewise-smooth image as

$$u = \sum_{i=1}^N c_i \chi_{\Omega_i} + b$$

where χ_{Ω_i} is the characteristic function of Ω_i , $i = 1, \dots, n$

$$\chi_{\Omega_i}(x) = \begin{cases} 1 & \text{if } x \in \Omega_i, \\ 0 & \text{if } x \in \Omega \setminus \Omega_i \end{cases}$$

- Based on the above image model, Le and Vese ([Le and Vese'07](#)) proposed a piecewise smooth segmentation model

$$\begin{aligned} \min_{c, b, \phi} \sum_{1 \leq j \leq m} \alpha \int_{\Omega} |\nabla H(\phi_j)| + \frac{\mu_1}{2} \int_{\Omega} |\nabla b|^2 dx + \frac{\mu_2}{2} \int_{\Omega} |D^2 b|^p dx \\ + \sum_{1 \leq i \leq n=2^m} \int_{\Omega} |v - c_i - b|^2 M_i(\phi(x)) dx \end{aligned}$$

- Related works such as ([Gu et al. '13](#)) and ([Jung'17](#)) etc..

PIECEWISE-SMOOTH MS MODELS

- Define a piecewise-smooth image as

$$u = b \sum_{i=1}^N c_i \chi_{\Omega_i}$$

- Based on the above image model, Li (Li et al '11) proposed a piecewise smooth segmentation model

$$\begin{aligned} \min_{c, b, \phi} \sum_{1 \leq j \leq m} \alpha \int_{\Omega} |\nabla H(\phi_j)| + \frac{\nu}{2} \int_{\Omega} (|\nabla \phi| - 1)^2 dx \\ + \sum_{1 \leq i \leq n=2^m} \int_{\Omega} \int_{\Omega} K(y-x) |v(x) - b(y)c_i|^2 dy M_i(\phi(x)) dx \end{aligned}$$

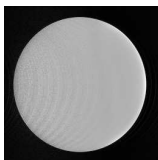
- Related works including (Li et al. '08, 09, 14) etc..

L0MS MODEL

- **Phantom MRI data:** Bruker 9.4 T, protocol: TurboRare_T2, pixel spacing of $0.12 \text{ mm} \times 0.12 \text{ mm} \times 1 \text{ mm}$



(a) v



(b) u



(c) b

- The image model is

$$v(x) = u(x)b(x) + n(x),$$

- Most existing methods require **the number of regions** in advance
- We aim to propose a **fast, accurate and robust** method

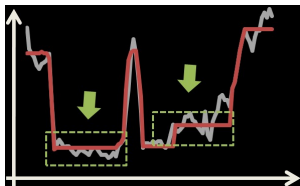
PIECEWISE CONSTANT REGULARIZATION

- We introduce the L_0 **gradient minimization** to regularize the piecewise constant function u , which is defined as

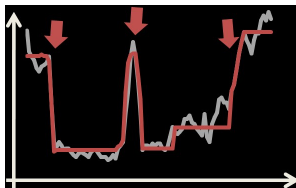
$$\|\nabla \hat{u}\|_0 = \#\{ p \mid |\partial_x \hat{u}_p| + |\partial_y \hat{u}_p| \neq 0 \},$$

where $\#\{\}$ is the counting operator, outputting the number of p that satisfies $|\partial_x \hat{u}_p| + |\partial_y \hat{u}_p| \neq 0$.

- **Two features:**
 - **flattening insignificant details** by removing small non-zero gradients
 - **enhancing prominent edges** since large gradients receive the same penalty as small ones



(a)



(b)

L_0 REGULARIZED MUMFORD-SHAH (L0MS)

- We obtain the **smooth regularization** for \hat{b} from Mumford-Shah model

$$S(\hat{b}) = \|\nabla \hat{b}\|^2$$

- We modify the **data fidelity** using the properties of local intensities as follows

$$\mathcal{E}(\hat{u}, \hat{f}) = \sum_{p \in \Omega} \left(\sum_{q \in \mathcal{N}_p} K(x_p - x_q) (\hat{v}_q - \hat{u}_q - \hat{b}_p)^2 \right)$$

where K is introduced as a nonnegative weighting function and $K(x_p - x_q) = 0$ for $q \notin \mathcal{N}_p$.

- We come up with the following **objective minimization problem**

$$\min_{\hat{u}, \hat{b}} \frac{1}{2} \mathcal{E}(\hat{u}, \hat{b}) + \alpha \|\nabla \hat{u}\|_0 + \frac{\mu}{2} \|\nabla \hat{b}\|^2 + \frac{\gamma}{2} \|\hat{b}\|^2$$

THE SOLUTION OF MINIMIZATION PROBLEM

- We introduce auxiliary variables (p, q) and rewrite the minimization problem as

$$\begin{aligned} \min_{\hat{u}, \hat{b}, p, q} \quad & \frac{1}{2} \mathcal{E}(\hat{u}, \hat{b}) + \alpha C(p, q) + \frac{\mu}{2} \|\nabla \hat{b}\|^2 + \frac{\gamma}{2} \|\hat{b}\|^2 \\ \text{s.t.}, \quad & p = \partial_x \hat{u}, \quad q = \partial_y \hat{u}, \end{aligned}$$

- We solve the constrained minimization problem using the **penalty method**

$$\begin{aligned} \min_{\hat{u}, \hat{b}, p, q} \quad & \left\{ \underbrace{\frac{1}{2} \mathcal{E}(\hat{u}, \hat{b})}_{\text{data fidelity}} + \underbrace{\frac{\mu}{2} \|\nabla \hat{b}\|^2 + \frac{\gamma}{2} \|\hat{b}\|^2}_{\text{smooth regularizer}} \right. \\ & \left. + \underbrace{\alpha C(p, q) + \frac{\beta}{2} (\|\partial_x \hat{u} - p\|^2 + \|\partial_y \hat{u} - q\|^2)}_{\text{piecewise constant regularizer}} \right\} \end{aligned}$$

ALGORITHM OF L0MS MODEL

- **Input:** image v , parameters $\alpha, \mu, \gamma, \beta_0, \beta_{max}$ and rate κ
- **Initialization:** $\hat{u}^{(0)} \leftarrow \hat{v}, \beta \leftarrow \beta_0, i \leftarrow 0$
- **Repeat**

- With $\hat{u}^{(i)}$, solve for $\hat{b}^{(i)}$ from

$$\hat{b}^{(i)} = \arg \min_{\hat{b}} \frac{1}{2} \mathcal{E}(\hat{u}^{(i)}, \hat{b}) + \frac{\gamma}{2} \|\hat{b}\|^2 + \frac{\mu}{2} \|\nabla \hat{b}\|^2,$$

which can be solved by FFT.

- With $\hat{u}^{(i)}$, solve for $p^{(i)}$ and $q^{(i)}$ from

$$(p^{(i)}, q^{(i)}) = \arg \min_{p, q} \alpha C(p, q) + \frac{\beta}{2} (\|\partial_x \hat{u}^{(i)} - p\|^2 + \|\partial_y \hat{u}^{(i)} - q\|^2),$$

which has the closed-form solution.

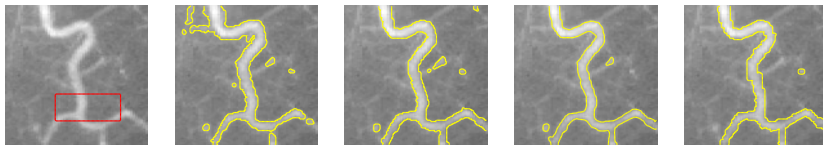
- With $\hat{b}^{(i)}, p^{(i)}$ and $q^{(i)}$, solve for $\hat{u}^{(i+1)}$ from

$$\hat{u}^{(i+1)} = \arg \min_{\hat{u}} \frac{1}{2} \mathcal{E}(\hat{u}, \hat{b}^{(i)}) + \frac{\beta}{2} (\|\partial_x \hat{u} - p^{(i)}\|^2 + \|\partial_y \hat{u} - q^{(i)}\|^2),$$

which can be solved by FFT.

- **until** $\beta \geq \beta_{max}$
- **Output:** \hat{u} and \hat{b}

COMPARISONS WITH OTHER VARIATIONAL MODELS



(a) Input

(b) TSMS

(c) BCFCM

(d) LIC

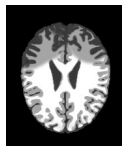
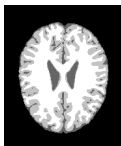
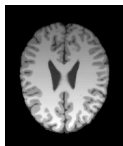
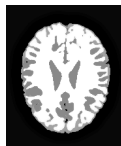
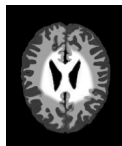
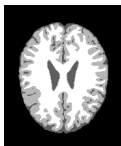
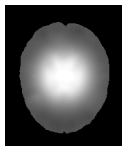
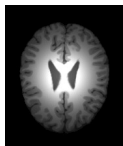
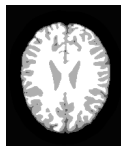
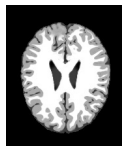
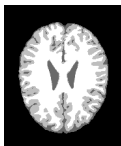
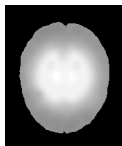
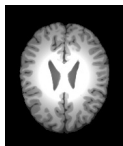
(e) LOMS

TSMS X. Cai, R. Chan, and T. Zeng, A two-stage image segmentation method using a convex variant of the Mumford-Shah model and thresholding, SIAM J. Imag. Sci., vol. 6, no. 1, pp. 368-390, 2013.

BCFCM M. N. Ahmed, S. M. Yamany, N. Mohamed, A. A. Farag, and T. Moriarty, A modified fuzzy c-means algorithm for bias field estimation and segmentation of MRI data, IEEE Trans. Med. Imag., vol. 21, no. 3, pp. 193-199, 2002.

LIC C. Li, R. Huang, Z. Ding, J. C. Gatenby, D. N. Metaxas, and J. C. Gore, A level set method for image segmentation in the presence of intensity inhomogeneities with application to MRI, IEEE Trans. Image Process., vol. 20, no. 7, pp. 2007-2016, 2011.

MR IMAGES WITH DIFFERENT BIAS PROFILES



(a) Input

(b) Bias field

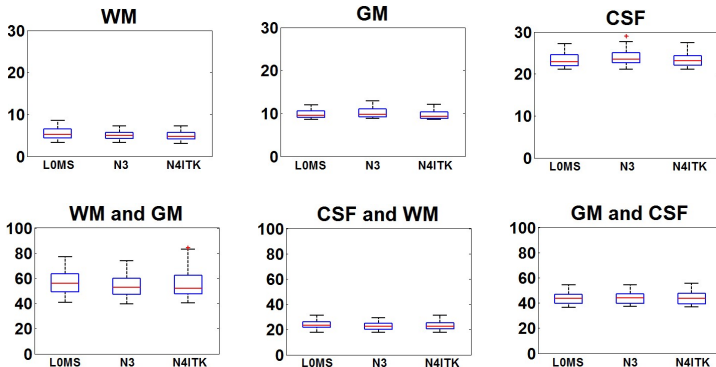
(c) L0MS

(d) BCFCM

(e) LIC

COMPARISON WITH BRAIN SOFTWARE TOOLS

- Comparison of bias correction with **N3** and **N4ITK** in terms of **Coefficient of Variation (CV)** and **Coefficient of Joint Variation (CJV)**

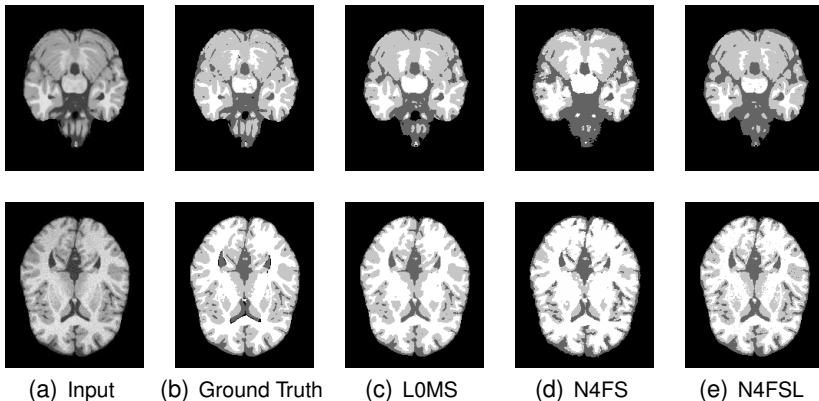


N3 J. G. Sled, A. P. Zijdenbos, and A. C. Evans, A nonparametric method for automatic correction of intensity nonuniformity in MRI data, IEEE Trans. Med. Imag., vol. 17, no. 1, pp. 87-97, 1998.

N4ITK N. J. Tustison, B. B. Avants, P. A. Cook, Y. Zheng, A. Egan, P. A. Yushkevich, and J. C. Gee, N4itk: improved N3 bias correction, IEEE Trans. Med. Imag., vol. 29, no. 6, pp. 1310-1320, 2010.

COMPARISON WITH BRAIN SOFTWARE TOOLS

- Visual comparison of brain segmentation with **FreeSurfer** and **FSL**, the input data of FreeSurfer and FSL are bias corrected data using N4ITK

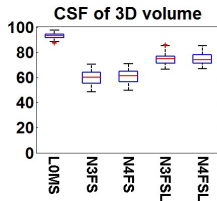
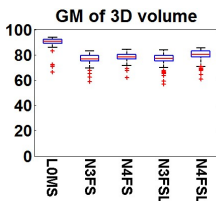
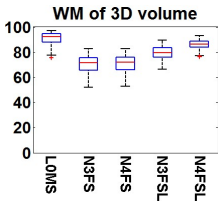
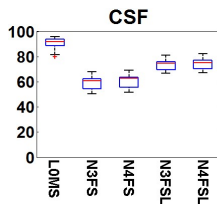
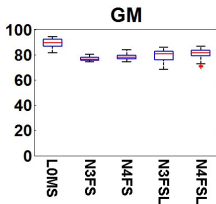
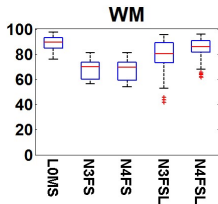


FreeSurfer <http://freesurfer.net/>

FSL <http://www.fmrib.ox.ac.uk/fsl/>

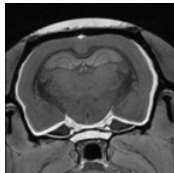
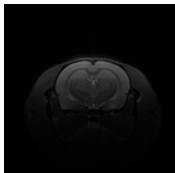
COMPARISON WITH BRAIN SOFTWARE TOOLS

- Comparison of brain segmentation with **FreeSurfer** and **FSL** in terms of **Jaccard Similarity (JS)**



RODENT BRAIN MRI

- Rodent brains have been used as preclinical models to investigate brain development, disease progression and new drug discovery etc.
- 1.5 T vs 3 T MRI systems:
 - increased **signal to noise ratio**;
 - increased **spatial resolution**;
 - increased **temporal resolution**;
 - increased **specific absorption rate**;
 - increased **acoustic noise**;
- **High-field MRI** is a popular technique for the study of rodent brains, e.g., 4.7 T, 9.4 T, 17.6 T etc.



(a) $256 \times 256 \times 26$ (b) $320 \times 320 \times 512$

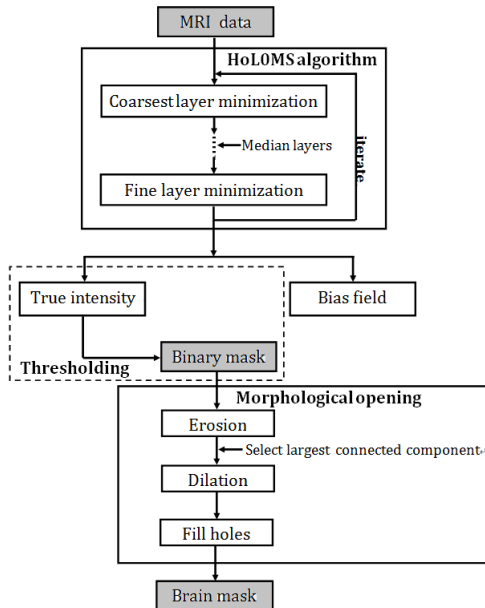
Severe intensity inhomogeneity exists in low-resolution MRI

L_0 AND HIGH-ORDER MUMFORD-SHAH MODEL

- **Observations** of LOMS:
 - The EL equation of $\mathcal{E}(\hat{u}, \hat{b})$ w.r.t. $\hat{b} \rightarrow \hat{\tilde{b}} = K * (\hat{v} - \hat{u})$;
 - The EL equation of $\|\nabla \hat{b}\|^2 \rightarrow \Delta \hat{\tilde{b}} = 0$;
- The two terms share the same functions on \hat{f}
- The high-order and L_0 regularized Mumford-Shah (**HoLOMS**) model

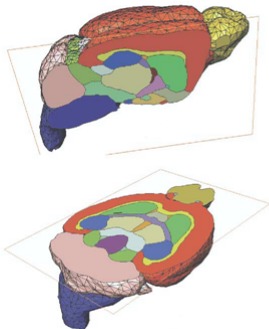
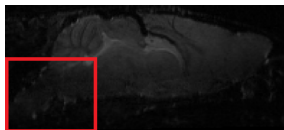
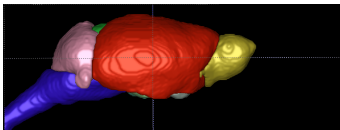
$$\min_{\hat{u}, \hat{b}} \frac{1}{2} \|\hat{v} - \hat{u} - \hat{b}\|^2 + \frac{\mu}{2} \|\nabla^2 \hat{b}\|^2 + \frac{\tau}{2} \|\hat{b}\|^2 + \alpha \|\nabla \hat{u}\|_0$$

MULTI-RESOLUTION BASED ALGORITHM



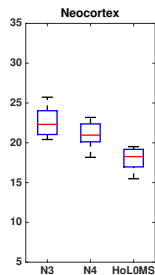
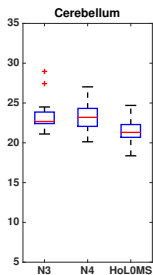
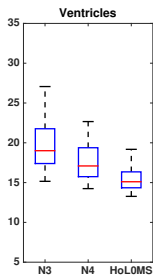
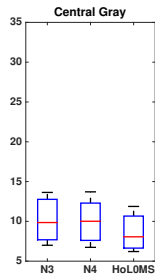
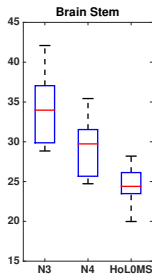
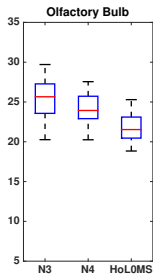
17.6 T MOUSE DATA SET

- Bruker 17.6 T; slice thickness of 0.1 mm; resolution $192 \times 96 \times 256$; 12 volumes

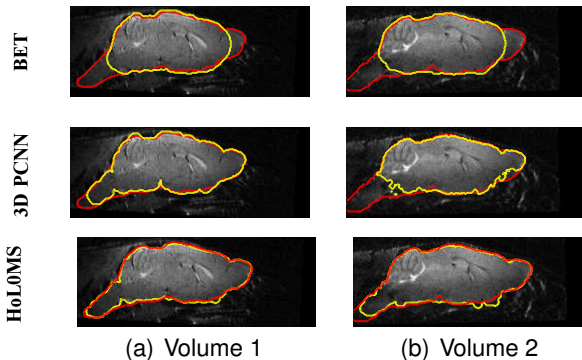


- Hippocampus
- External_capsule
- Caudate_putamen
- Ant_commissure
- Globus_pallidus
- Internal_Capsule
- Thalamus
- Cerebellum
- Superior_colliculi
- Ventricles
- Hypothalamus
- Inferior_colliculi
- Central_gray
- Neocortex
- Amygdala
- Olfactory_bulb
- Brain_stem
- Rest_of_Midbrain
- BasalForebrain_Septum
- Fimbria

BIAS CORRECTION EVALUATION



BRAIN EXTRACTION EVALUATION



BET S. M. Smith, Fast robust automated brain extraction, Human Brain Mapping, vol. 17, no. 3, pp. 143-155, 2002.

3D PCNN N. Chou, J. Wu, J. B. Bingren, A. Qiu, and K. H. Chuang, Robust automatic rodent brain extraction using 3-d pulse-coupled neural networks (PCNN), IEEE Transactions on Image Processing, vol. 20, no. 9, pp. 2554-2564, 2011.

RICIAN NOISE

- MRI scanner acquires complex data as follows

$$S = S_R + iS_I = u + \eta_1 + i\eta_2,$$

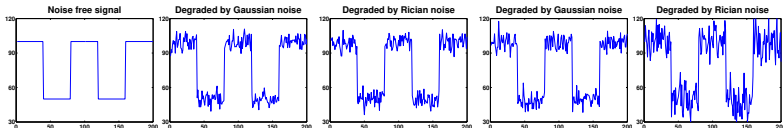
where u is the true amplitude of the image, $\eta_1, \eta_2 \sim \mathcal{N}(0, \sigma^2)$.

- The magnitude image f is expressed as

$$f = \sqrt{(v + \eta_1)^2 + \eta_2^2}$$

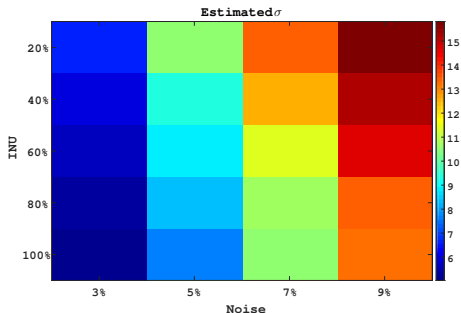
- The probability density function of f follows the Rician distribution

$$p(f|v) = \frac{f}{\sigma^2} e^{-\frac{v^2+f^2}{2\sigma^2}} I_0\left(\frac{vf}{\sigma^2}\right)$$



NOISE ESTIMATION

- The estimated noise is affected by true noise level and intensity nonuniformity



THE MAP MODEL

- The MAP gives: $\hat{v} = \arg \max_v P(v|f) = \arg \max_v \frac{P(f|v)P(v)}{P(f)}$
- The likelihood term is determined by Rician distribution

$$G(v) := -\log(P(f|v)) = \int_{\Omega} \frac{1}{2\sigma^2} v^2(x) - \log I_0\left(\frac{f(x)v(x)}{\sigma^2}\right) dx$$

- Assume v follows a TV prior

$$P(v) \propto \exp(-\alpha \int_{\Omega} |\nabla v| dx)$$

- Meanwhile, we have $v = ub$, where u follows a TV prior, and b is spatially smooth, i.e., its derivative being square integrable

$$P(u) \propto \exp(-\beta \int |\nabla u| dx), \quad \text{and} \quad P(b) \propto \exp(-\frac{\gamma}{2} \int |\nabla b|^2 dx),$$

- We arrive at

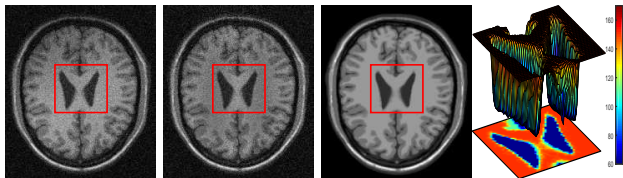
$$\min_{\substack{0 \leq v \leq 255 \\ 0 \leq u \leq 255, b}} G(v) + \frac{\lambda}{2} \|v - ub\|_2^2 + \alpha \|\nabla v\|_1 + \beta \|\nabla u\|_1 + \frac{\gamma}{2} \|\nabla b\|_2^2$$

ALGORITHM OF NNC MODEL

1. Initialization: v^0, u^0, b^0 ;
2. For $k = 0, 1, \dots$: compute v^{k+1}, u^{k+1} and b^{k+1} from
 - $v^{k+1} = \arg \min_{0 \leq v \leq 255} G(v) + \frac{\lambda}{2} \|v - u^k b^k\|_2^2 + \alpha \|\nabla v\|_1$,
which can be solved by primal-dual scheme.
 - $u^{k+1} = \arg \min_{0 \leq u \leq 255} \frac{\lambda}{2} \|v^{k+1} - u b^k\|_2^2 + \beta \|\nabla u\|_1$,
which can be solved by primal-dual scheme.
 - $b^{k+1} = \arg \min_b \frac{\lambda}{2} \|v^{k+1} - u^{k+1} b\|_2^2 + \frac{\gamma}{2} \|\nabla b\|_2^2$,
which can be solved by FFT.
3. Measure the relative residuals and stop iteration if they are small than the tolerance

$$\max\left(\frac{\|u^{k+1} - u^k\|_2^2}{\|u^{k+1}\|_2^2}, \frac{\|b^{k+1} - b^k\|_2^2}{\|b^{k+1}\|_2^2}\right) \leq tol.$$

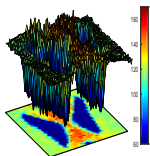
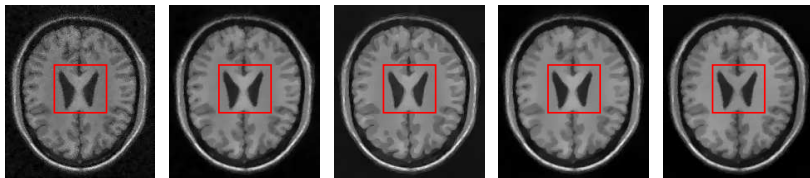
NUMERICAL RESULTS



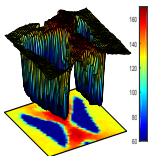
(a) Input

(b) N4

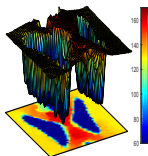
(c) Ground truth



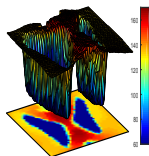
(d) MSE



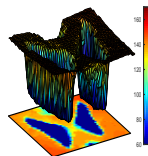
(e) TVM



(f) LGTV



(g) CTV



(h) NNC



NUMERICAL RESULTS

Table: PSNR, MSSIM and CV of white matter of T_1 -weighted MRI data with different noise and 100% INU. N4 denotes the image corrected by N4 bias correction method.

Methods	5%			7%			9%		
	PSNR	MSSIM	CV	PSNR	MSSIM	CV	PSNR	MSSIM	CV
Original	19.2471	0.7507	12.9733	18.2573	0.6966	14.8417	17.7518	0.6540	16.5297
N4	22.8128	0.7935	9.6305	20.8579	0.7393	12.2887	19.5991	0.6893	14.4233
MSE	23.6754	0.8224	7.6191	22.0643	0.7893	8.7053	21.1621	0.7628	9.1400
TVM	25.3463	0.8542	6.5555	24.8452	0.8410	7.2671	24.7781	0.8288	7.3330
LGTV	23.8220	0.8193	6.1189	23.2543	0.8086	6.6827	22.6086	0.7905	7.6223
CTV	25.4766	0.8587	6.4084	25.2772	0.8423	6.9673	24.9513	0.8335	7.2977
NNC	26.7647	0.8854	5.9724	25.8621	0.8666	6.5322	25.4807	0.8571	6.9881

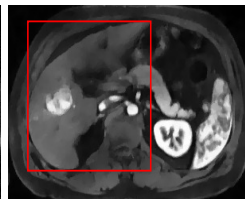
NUMERICAL RESULTS



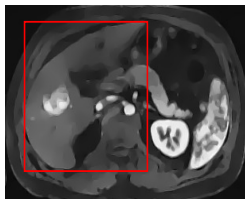
(a) Original image



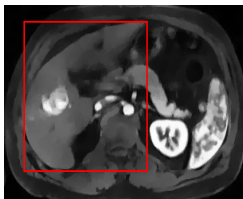
(b) MSE



(c) TVM



(d) LGTV



(e) CTV



(f) NNC

NUMERICAL RESULTS



(a) Original image



(b) MSE



(c) TVM



(d) LGTV

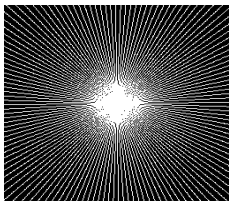


(e) CTV

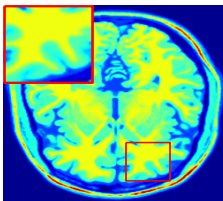


(f) NNC

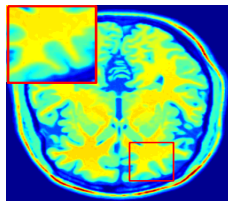
MR RECONSTRUCTION WITH BIAS CORRECTION



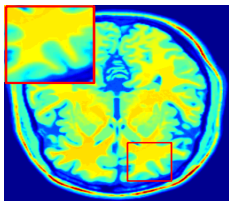
(a) k -space Data



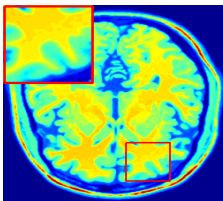
(b) Ground Truth



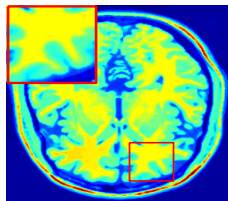
(c) PANO



(d) BM3D

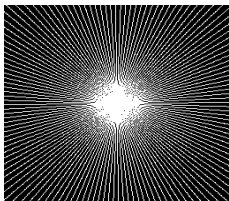


(e) TGV+Shearlet

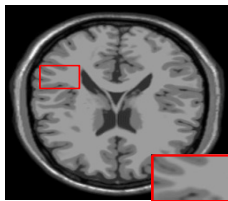


(f) Proposed

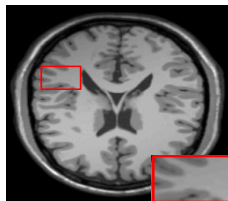
MR RECONSTRUCTION WITH BIAS CORRECTION



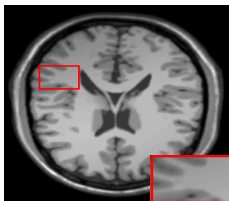
(a) k -space Data



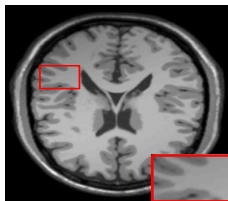
(b) Ground Truth



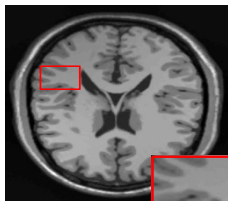
(c) PANO



(d) BM3D



(e) TGV+Shearlet



(f) Proposed

Thank you!